

General equation for the determination of the crystallite size L_a of nanographite by Raman spectroscopy

L. G. Cançado,^{a)} K. Takai, and T. Enoki

Department of Chemistry, Tokyo Institute of Technology, 2-12-1 Ookayama, Meguro-ku, Tokyo 152-8551, Japan

M. Endo, Y. A. Kim, and H. Mizusaki

Faculty of Engineering, Shinshu University, 4-17-1 Wakasato, Nagano-shi 380-8553, Japan

A. Jorio, L. N. Coelho, R. Magalhães-Paniago, and M. A. Pimenta

Departamento de Física, Universidade Federal de Minas Gerais, 30123-970 Belo Horizonte, Brazil

(Received 30 December 2005; accepted 4 March 2006; published online 19 April 2006)

This work presents a systematic study of the ratio between the integrated intensities of the disorder-induced D and G Raman bands (I_D/I_G) in nanographite samples with different crystallite sizes (L_a) and using different excitation laser energies. The crystallite size L_a of the nanographite samples was obtained both by x-ray diffraction using synchrotron radiation and directly from scanning tunneling microscopy images. A general equation for the determination of L_a using any laser energy in the visible range is obtained. Moreover, it is shown that I_D/I_G is inversely proportional to the fourth power of the laser energy used in the experiment. © 2006 American Institute of Physics. [DOI: 10.1063/1.2196057]

Raman spectroscopy has been widely used in the last four decades to characterize nanographitic systems, such as pyrolytic graphite, carbon fibers, glassy carbon, nanographite ribbons, and carbon nanotubes.^{1,2} The Raman spectrum of a crystalline graphite has only one Raman peak at 1580 cm^{-1} , which is called the G band. However, in the case of samples with some structural disorder that breaks the translational symmetry (e.g., impurities, edges, finite size effects, etc.) an additional feature can be observed at 1350 cm^{-1} for excitation laser energy of 2.41 eV , and it is usually called the D band.^{3,4}

In 1970, Tuinstra and Koenig^{3,4} performed systematic Raman and x-ray diffraction studies of many graphitic samples with different in-plane crystallite sizes L_a and concluded that the ratio of the D and G band intensities (I_D/I_G) was inversely proportional to the crystallite sizes L_a , which were obtained from the width of the x-ray diffraction peaks. Knight and White later summarized the Raman spectra of various graphite systems measured using the $\lambda=514.5\text{ nm}$ ($E_l=2.41\text{ eV}$) laser line and derived an empirical expression which allows the determination of L_a from the (I_D/I_G) ratio.⁵ Later on, Mernagh *et al.*⁶ showed that the ratio I_D/I_G depends strongly on the excitation laser energy (E_l) used in the Raman experiment, revealing that the Knight and White empirical formula was only valid when the experiment was done using the $\lambda=514.5\text{ nm}$ ($E_l=2.41\text{ eV}$) laser line. Despite the fact that the empirical relation relating L_a and I_D/I_G has been widely applied to characterize the nanographitic structures, there is no report until now generalizing this relation for Raman experiments performed with different excitation laser energies. In this work, a general formula that gives the crystallite size L_a of nanographitic systems for any excitation laser energy in the visible range is presented. This result is specially important since recent fabrication techniques of graphite nanostructures allowed the observation of the quan-

tum Hall effect in a single layer of graphene.^{7,8}

The samples used in the experiment were diamondlike carbon (DLC) films with thicknesses of several microns, heat treated at different temperatures and, thus, giving rise to nanographites with different L_a values. The films were prepared by a pulsed laser deposition method using a highly oriented pyrolytic graphite target in vacuum conditions (5×10^{-6} Torr). The heat treatment was made using an electrical furnace setup, at heat treatment temperatures (HTTs) of $1800, 2000, 2200, 2300, 2400, 2600,$ and $2700\text{ }^\circ\text{C}$. During the heat treatment process, the samples were kept inside a closed graphite tube, under an inert gas atmosphere (argon with 99.999% of purity) flowing at 1 l/min . Before heat treatment, the sp^3 and sp^2 carbon phases coexist in the samples, but the sp^3 phases completely disappear for heat treatment temperatures above $1600\text{ }^\circ\text{C}$.⁹ Therefore, the samples used in this work correspond to aggregates of nanographite crystals.

Raman scattering experiments were performed at room temperature using a triple monochromator micro-Raman spectrometer (Dilor XY) using the following laser energies (wavelengths): krypton of 1.92 eV (647 nm) and 2.18 eV (568 nm), and argon of 2.41 eV (514.5 nm), 2.54 eV (488 nm), and 2.71 eV (457.9 nm). The laser power density was always less than 10^5 W/cm^2 . The x-ray diffraction measurements were performed in the transmission ($\theta/2\theta$) geometry. The energy of the synchrotron radiation used was 10.0 keV ($\lambda=0.120\text{ nm}$). The transmission geometry was used since the (100) direction lies on the sample surface. Scanning tunneling microscopy (STM) measurements were performed using a Nanoscope II MultiMode microscope from Digital Instruments.

Figure 1(a) shows the STM images of the samples obtained at different heat treatment temperatures. The evolution of the crystallite sizes with increasing heat treatment temperature is clearly observed from the STM images. The grain boundaries are very clear, and the samples present good

^{a)}Electronic mail: luizgustavocancado@yahoo.com.br

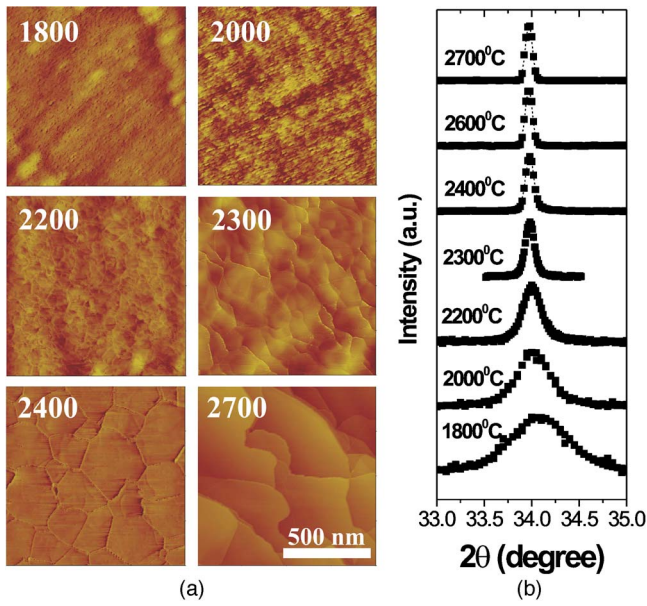


FIG. 1. (Color online) (a) STM images of the sample heat treated at different temperatures. All images are shown in the same scale ($1 \times 1 \mu\text{m}^2$). (b) X-ray diffraction profile of the (100) peak for samples heat treated at different temperatures.

structural homogeneity. A high resolution STM analysis shows that the c axis is always perpendicular to the sample surface.

Figure 1(b) shows the evolution of the (100) x-ray diffraction peak obtained using synchrotron radiation, for the samples heat treated at different temperatures. The crystallite size L_a was obtained by evaluating the Scherrer relation $L_a = 1.84\lambda / \beta \cos \theta$, where λ is the synchrotron radiation wavelength (0.120 nm), θ is the position of the (100) peak, and β is the half-height width of the (100) peak of graphite in 2θ (rad) units.¹⁰ To avoid the intrinsic instrumental broadening, the β parameter was corrected using the equation $\beta = \sqrt{\beta_m^2 - \beta_{Si}^2}$, where β_m is the half-height width of the measured (100) peak of the samples, and β_{Si} is the half-height width of the (220) peak of a standard silicon sample obtained experimentally.

The analysis of x-ray diffraction profiles is the usual and standard way to measure the crystallite size of nanocrystals. However, this is an indirect measurement and the results can be modified by different factors, such as the asymmetric profile of the peak and the low resolution of the x-ray diffraction setup. In the present case, we have used a high resolution synchrotron x-ray apparatus, and the diffraction peaks are quite symmetric. The mean crystallite sizes were also obtained directly from the STM images and are in good agreement with the L_a parameter obtained by x-ray diffraction (see Table I).

Figure 2 shows the Raman spectra of the D , G , and D' bands of the sample heat treated at 2000 °C, for five different laser energy values (1.92, 2.18, 2.41, 2.54, and 2.71 eV). The origin and dispersive behavior of the D and D' bands shown in Fig. 2 were explained by the double resonance Raman mechanism in graphite.^{11–13} Notice that the ratio (I_D/I_G) is strongly dependent on the excitation laser energy. Therefore, it is clear that the empirical formula proposed by Knight and White⁵ for the determination of L_a from the I_D/I_G ratio must be generalized for other excitation laser energies. The ratio of the D' (centered at 1620 cm^{-1}) and G band

TABLE I. L_a values of the heat treated samples obtained by x-ray diffraction analysis and from the STM images.

HTT (°C)	L_a (nm)	
	(X ray)	(STM)
2700	490	550
2600	340	300
2400	190	220
2300	150	120
2200	65	60
2000	35	40
1800	20	20

intensities also exhibits an interesting and particular laser energy dependency, which will be discussed elsewhere.

Figure 3(a) shows the plot of the integrated intensities of the D and G bands (I_D/I_G) vs $1/L_a$ for all samples and laser energies used in the experiment. In order to collapse the different straight lines in a single one, the experimental values I_D/I_G were multiplied by different powers of E_l , and the best result was obtained when we multiplied I_D/I_G by the fourth power of the excitation laser energy (E_l^4). Figure 3(b) shows that all experimental points collapse in the same straight line in the $(I_D/I_G)E_l^4$ vs $1/L_a$ plot. By fitting the data depicted in Fig. 3(b), a general expression that gives the L_a crystallite size from the integrated intensity ratio I_D/I_G by using any laser line in the visible range can be obtained and is given by

$$L_a(\text{nm}) = \frac{560}{E_l^4} \left(\frac{I_D}{I_G} \right)^{-1}, \quad (1)$$

where E_l is the excitation laser energy used in the Raman experiment in eV units. Considering the laser line wavelength (λ_l) in nanometer units, Eq. (1) can be rewritten as

$$L_a(\text{nm}) = (2.4 \times 10^{-10}) \lambda_l^4 \left(\frac{I_D}{I_G} \right)^{-1}. \quad (2)$$

The constant of proportionality between L_a and $(I_D/I_G)^{-1}$ obtained from Eqs. (1) and (2) by using $E_l = 2.54 \text{ eV}$ (13.5 nm) is higher than that reported by Knight and White (4.4 nm).⁵ First, we have considered here the integrated intensities (areas) of the D and G bands instead of using the ratio of the peak amplitudes, as in Refs. 3 and 4. On the other

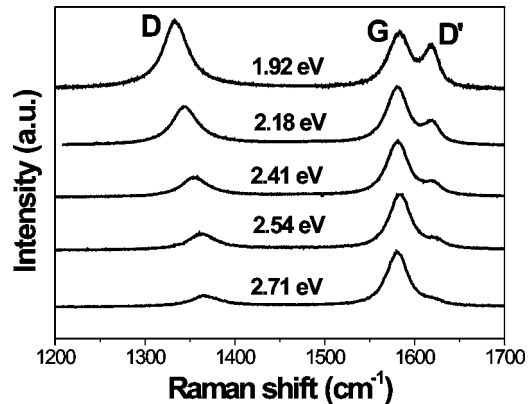


FIG. 2. (Color online) Raman spectra of the sample heat treated at 2000 °C, for five different laser energy values (1.92, 2.18, 2.41, 2.54, and 2.71 eV).

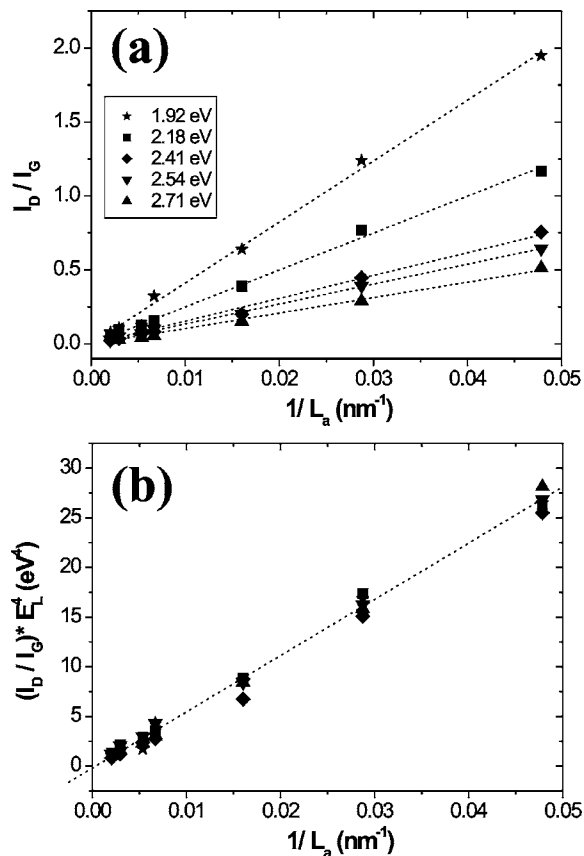


FIG. 3. (Color online) (a) Plot of the ratio of the integrated intensities of the D and G bands (I_D/I_G) vs $1/L_a$ for all spectra obtained with the five different excitation laser energies. (b) All experimental results shown in part (a) collapse in the same straight line in the $(I_D/I_G)E_l^4$ vs $1/L_a$ plot.

hand, different values of the proportionality constant can also be ascribed to the instrumental width of the x-ray diffraction peaks obtained from different x-ray sources or to a broad distribution of crystallite sizes in different samples. In the present study, the width of the Raman D band is very narrow, reflecting the narrow distribution of crystallite sizes. It must be stressed that Eqs. (1) and (2) are certainly valid in the range of laser energies used in this work (visible range).

In summary, a systematic analysis of the dependence of the ratio between the integrated intensities of the D and G

bands (I_D/I_G) on the crystallite size and on the excitation laser energy is presented. The crystallite sizes L_a of nanographite samples were obtained by x-ray diffraction using synchrotron radiation and directly from scanning tunneling microscopy images. Resonant Raman spectroscopy was performed using five excitation laser energies in the visible range. From the analysis of the experimental results, a general formula that allows the determination of the crystallite size L_a by Raman spectroscopy using any excitation laser energy E_l in the visible range is obtained. We also show that, for a given sample, I_D/I_G is inversely proportional to E_l^4 . A theory that takes into account the E_l dependence of all matrix elements involved in the Raman process, giving rise to the D and G bands, is needed to explain the dependence of (I_D/I_G) on E_l^4 .

This work was supported by Instituto de Nanociências–MCT and FAPEMIG. One of the authors (L.G.C.) acknowledges the support from the Brazilian Agency CNPq and from TIT during his visit to TIT, and the support from ABTLuz during his visit to Brazilian Synchrotron source.

¹M. S. Dresselhaus, G. Dresselhaus, K. Sugihara, I. L. Spain, and H. A. Goldberg, *Graphite Fibers and Filaments*, Springer Series in Material Science Vol. 5 (Springer, Berlin, 1988).

²R. Saito, M. S. Dresselhaus, and G. Dresselhaus, *Physical Properties of Carbon Nanotubes* (Imperial College Press, London, 1998).

³F. Tuinstra and J. L. Koenig, *J. Chem. Phys.* **53**, 1126 (1970).

⁴F. Tuinstra and J. L. Koenig, *J. Compos. Mater.* **4**, 492 (1970).

⁵D. S. Knight and W. White, *J. Mater. Res.* **4**, 385 (1989).

⁶T. P. Mernagh, Ralph P. Cooney, and Robert A. Johnson, *Carbon* **22**, 39 (1984).

⁷Y. Zhang, Y. W. Tan, H. L. Stormer, and P. Kim, *Nature (London)* **438**, 201 (2005).

⁸K. S. Noroselov, A. K. Geim, S. M. Morozov, D. Jiang, M. I. Katsnelson, I. V. Grigorieva, S. V. Dubonos, and A. A. Firsov, *Nature (London)* **438**, 197 (2005).

⁹Kazuyuki Takai, Meigo Oga, Hirohiko Sato, Toshiaki Enoki, Yoshimasa Ohki, Akira Taomoto, Kazutomo Suenaga, and Sumio Iijima, *Phys. Rev. B* **67**, 214202 (2003).

¹⁰Mohindar S. Seehra and Arthur S. Pavlovic, *Carbon* **31**, 557 (1992).

¹¹A. V. Baranov, A. N. Bekhterev, Y. S. Bobovich, and V. I. Petrov, *Opt. Spectrosc.* **62**, 612 (1987).

¹²C. Thomsen and S. Reich, *Phys. Rev. Lett.* **85**, 5214 (2000).

¹³R. Saito, A. Jorio, A. G. Souza Fiho, G. Dresselhaus, M. S. Dresselhaus, and M. A. Pimenta, *Phys. Rev. Lett.* **88**, 027401 (2002).